

## Effects of Heat Input on Pitting Corrosion in Super Duplex Stainless Steel Weld Metals

Yong taek Shin<sup>1</sup>, Hak soo Shin<sup>1</sup>, and Hae woo Lee<sup>2,\*</sup>

<sup>1</sup>Samsung Heavy Industries Co.,Ltd, Department of Material Research,  
Geoje-si 656-710, Gyoungnam, Korea

<sup>2</sup>Dong-A University, Department of Materials Science and Engineering, Hadan-dong,  
Busan 604-714, Korea

(received date: 21 November 2011 / accepted date: 6 February 2012)

Due to the difference in reheating effects depending on the heat input of subsequent weld passes, the microstructure of the weld metal varies between acicular type austenite and a mixture of polygonal type and grain boundary mixed austenite. These microstructural changes may affect the corrosion properties of duplex stainless steel welds. This result indicates that the pitting resistance of the weld can be strongly influenced by the morphology of the secondary austenite phase. In particular, the ferrite phase adjacent to the acicular type austenite phase shows a lower Pitting Resistance Equivalent (PRE) value of 25.3, due to its lower chromium and molybdenum contents, whereas the secondary austenite phase maintains a higher PRE value of more than 38. Therefore, it can be inferred that the pitting corrosion is mainly due to the formation of ferrite phase with a much lower PRE value.

**Key words:** metals, welding, corrosion, scanning electron microscopy (SEM), grain boundary

### 1. INTRODUCTION

Duplex stainless steels have better corrosion resistance and mechanical properties than austenitic or ferritic stainless steels. Therefore, they have been commonly employed in corrosion resistant applications for many years, especially in the offshore industry. In addition, the newly developed duplex grade, such as super duplex stainless steel with a higher PRE of more than 35, is utilized for more severely corrosive environments [1,2]. However, it is known that phase transformations, such as sigma formation and the precipitation of chromium nitride and carbides, are favored when stainless steels are exposed to elevated temperatures in the range of 500-1000 °C [1]. For this reason, various investigations have been performed on the formation mechanism, or the effect on the corrosion resistance, of the tertiary phase in the heat affected zone or heat treated base material [3-5]. However, only limited research results are currently available regarding these pitting corrosion problems in the case of weld metal, because the properties of the weld metal can be changed drastically during the solidification phase and subsequent weld passes [6].

In the present study, the microstructure characteristics at

the weld root were investigated, to clarify the pitting corrosion properties according to the heat input of the subsequent weld pass in super duplex stainless steel welds.

### 2. EXPERIMENTAL PROCEDURES

The chemical composition of UNS S32760 Super Duplex Stainless Steel (SDSS) pipe is summarized in Table 1. Gas Tungsten Arc Welding (GTAW) with Ar+2% N<sub>2</sub> shielding gas, which is commonly used for joining thin pipe sections, was applied. The welding conditions are given in Table 2 and the macro section of the welded joint is presented in Fig. 1. To investigate the reheating effect of the subsequent weld passes on the microstructure, as well as the resulting pitting resistance, at the weld root, two different types of heat input in the second weld pass are considered, as shown in Table 2. The specimens were polished and electrolytic etched with 10% sodium hydroxide to compare the microstructural variation caused by the difference in heat inputs. Microstructural investigations were carried out using an optical microscope and a Scanning Electron Microscope (SEM) equipped with Energy Dispersive X-rays (EDX). The pitting resistance of the weld metal was assessed in accordance with ASTM G48 by immersion test at 40 °C for 24 h in 6% ferric chloride solution. After the pitting corrosion test, the weight loss of the specimens was measured and the main cause of the pit-

\*Corresponding author: hwlee@dau.ac.kr

**Table 1.** Chemical composition of the super duplex stainless steel studied (wt%)

	UNS/EN No.	C	Si	Mn	Cr	Ni	Mo	W	N	PRE <sup>1)</sup>
Base material	S32750	0.015	0.19	0.79	25.40	7.10	3.90	–	0.27	42.6
Filler material	25 9 4 N L	0.011	0.36	0.41	25.36	9.50	3.96	<0.01	0.23	42.1

<sup>1)</sup>PRE = wt% Cr + 3.3 x wt% Mo + 16 x wt%

**Table 2.** Gas tungsten arc welding process parameters

Specimen	Pass	Current (A)	Voltage (V)	Speed (mm/min)	Heat input (kJ/mm)
A	1st	100	10	50	1.20
	2nd	160	12	110	1.05
	3rd~	130	12	110	0.85
B	1st	100	10	50	1.20
	2nd	120	12	100	0.86
	3rd~	130	12	110	0.85

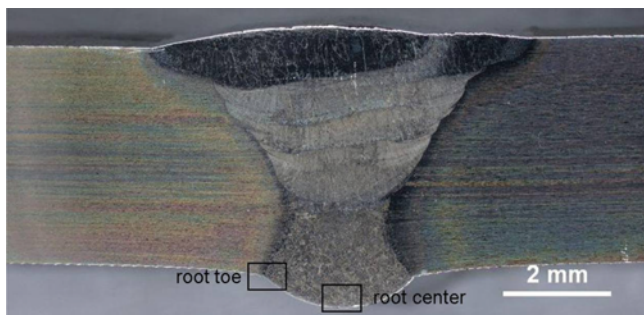


**Fig. 1.** Macro section of welded joint in the present study (square box on the section indicate microstructure observed region in each specimen).

ting corrosion in connection with the microstructure was investigated.

### 3. RESULTS AND DISCUSSION

#### 3.1. Metallography

The microstructures of specimens A and B, which were subjected to high and low heat inputs in the second weld pass, are shown in Figs. 2 and 3, respectively. In each specimen, the microstructure of the root center and root toe regions close to the surface of the weld root was observed, as indicated in Fig. 1. The observation of the morphology of the austenite in the weld root showed that the microstructural

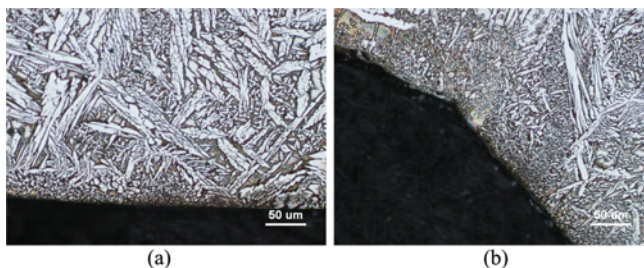


**Fig. 2.** Optical microstructure of root surface of specimen A; (a) root center and (b) root toe.

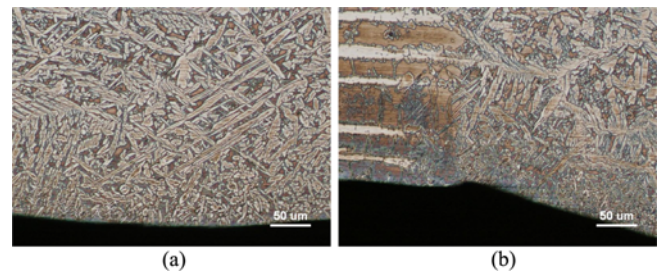


**Fig. 3.** Optical microstructure of root surface of specimen B; (a) root center and (b) root toe.

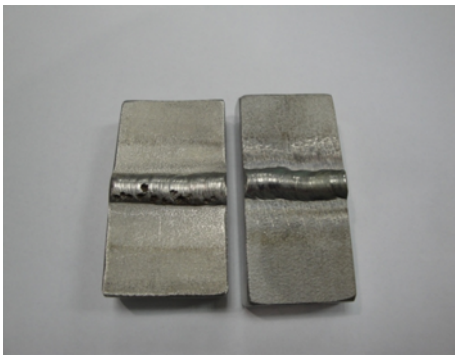
features of specimen A in the intragranular region, that is within the primary austenite ( $\gamma_1$ ), is mostly filled with acicular type secondary austenite ( $\gamma_2$ ) in both the root center and root toe. On the other hand, the microstructures of specimen B consist mainly of polygonal type and grain boundary austenite. As already reported by many researchers, the secondary austenite was transformed from the metastable ferrite phase, due to the reheating effect caused by the subsequent weld passes [5,7-8]. Therefore, it is recognized that the microstructural difference between the two specimens might contribute to the difference in the heat inputs during the subsequent welding passes. Due to the higher heat input of the second weld pass, the thickness of the welding deposit in specimen A after this pass is larger than that of specimen B. In other words, peak temperature at the root weld in specimen A is lower than that of specimen B during the third pass welding, so the root weld in specimen A was not sufficiently reheated by the third pass welding to form stable polygonal type secondary austenite, as shown in specimen B. Consequently, the acicular type secondary austenite of specimen A was considered to be formed by this insufficient reheating effect.

#### 3.2. Pitting corrosion test

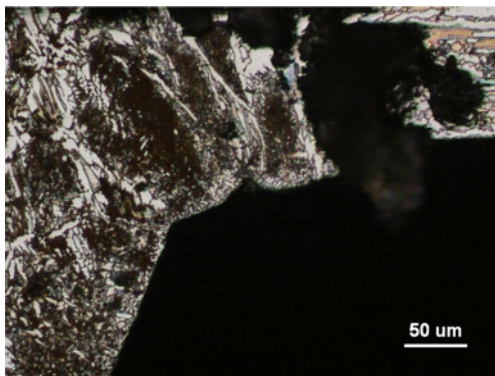
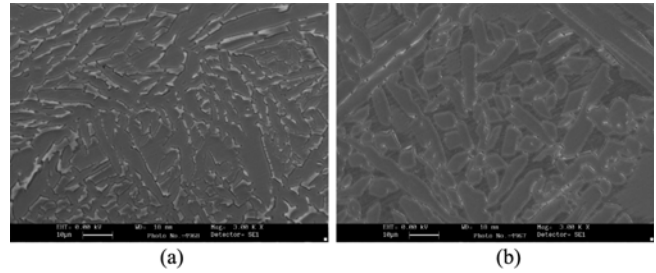
The pitting resistances of the specimens are presented in Table 3 and Fig. 4. It is observed that specimen A with a large amount of acicular type secondary austenite is severely

**Table 3.** Pitting corrosion test results by immersion in 6% ferric chloride solution at temperature of 40 °C for 24 h

Specimen	PRE		Pit location	Weight loss (g/m <sup>2</sup> )
	Base material	Filler material		
A	42.6	42.1	Root toe	39.68
B			–	0

**Fig. 4.** Photographs of pitting corrosion tested specimens (left is specimen A and right is specimen B).

pitted at the root surface, especially in the root toe region, as shown in Fig. 4. On the contrary, specimen B without any acicular type austenite phase is free from pitting corrosion and did not experience any substantial weight loss. Fig. 5 shows that the slightly pitted region of specimen A corresponds to the initial pitting stage. Generally, the formation of secondary austenite is known to be the main cause of pitting corrosion, because it has lower chromium, molybdenum and nitrogen contents than the pre-existing austenite, *i.e.* grain boundary austenite [9-13]. However, it is observed that the acicular type secondary austenite was not corroded, but that corrosion occurred mainly in the region of the ferrite phase between the secondary austenite phases. To verify the local weak zone from the viewpoint of its corrosion, chemical analysis using a SEM equipped with EDX was carried out for each phase in the root pass of specimen A. The second

**Fig. 5.** Slightly pitted region corresponds to initial pitting stage of specimen A (bright phases indicate austenite not attacked at initial pitting stage).**Fig. 6.** Scanning electron micrographs of specimen A; (a) root weld and (b) second pass weld.**Table 4.** Chemical compositions of each phase in root weld and second pass weld of specimen A (wt%)

Location	Phase	Cr	Ni	Mo	PRE
Root weld	$\gamma_2$	27.14	7.88	4.11	40.7
		26.81	8.62	3.54	38.5
	$\alpha$	16.10	9.97	2.80	25.3
		23.30	10.79	2.93	33.0
	$\gamma_2$	26.60	8.72	3.63	38.6
2nd pass weld	$\gamma_2$	26.98	8.31	3.59	38.8
		26.68	8.73	3.53	38.3
	$\gamma_1$	26.02	8.25	4.05	39.4
		27.09	8.33	4.41	41.6
$\alpha$	26.47	9.27	4.26	40.5	

pass weld deposits of the specimens, which have mainly a polygonal type secondary austenite, were analyzed in order to compare their corrosion properties. The microstructure of the root weld of specimen A is mainly composed of acicular type secondary austenite (dark) and ferrite phase (bright) between the austenite phases, as shown in Fig. 6. On the other hand, the second pass weld has island type polygonal austenite in the ferrite matrix. The contents of the principal elements that determine the corrosion resistance are given in Table 4. Against expectations, the PRE values of the secondary austenite in the weld root are relatively high, being over 38. However, the ferrite phase between the secondary austenite in the weld root has significantly lower chromium and molybdenum contents and, therefore, its PRE value is drastically decreased to 25.3. In this case, the ferrite phase could act as a preferential pitting initiation site when exposed to a corrosive environment. This result is also consistent with the microstructural feature of the initial pitting stage shown in Fig. 5. The reason for the decreased amounts of chromium and molybdenum in the ferrite is not clearly understood, and additional studies are necessary. In the second pass weld, all the ferrite, the primary and secondary austenite have higher PRE values, of over 38, which are different from that in the weld root. Figure 7 shows the distribution of the principal alloying elements across the secondary austenite and the ferrite phase in the weld root of specimen A. The content of chromium in the ferrite phase was remarkably decreased to



